OncoTargets and Therapy

Dovepress
Taylor & Francis Group

Open Access Full Text Article

ORIGINAL RESEARCH

lncSLERT Promotes Liver Metastasis in Colorectal Cancer by Down-Regulating HUNK Expression via RBM15-Mediated m6A Modification

Lin Wang[1,*], Liming Zhao[2,*], Jialiang Liu[2], Pu Cheng[2], Mingyu Han[3], Zhaoxu Zheng[2]

[1]The State Key Laboratory of Molecular Oncology, National Cancer Center/National Clinical Research Center for Cancer/Cancer Hospital, Chinese Academy of Medical Sciences and Peking Union Medical College, Beijing, 100021, People's Republic of China; [2]Department of Colorectal Surgery, National Cancer Center/National Clinical Research Center for Cancer/ Cancer Hospital, Chinese Academy of Medical Sciences and Peking Union Medical College, Beijing, People's Republic of China; [3]Department of Hepatobiliary Surgery, National Cancer Center/National Clinical Research Center for Cancer/ Cancer Hospital, Chinese Academy of Medical Sciences and Peking Union Medical College, Beijing, People's Republic of China

*These authors contributed equally to this work

Correspondence: Zhaoxu Zheng, Department of Colorectal Surgery, National Cancer Center/National Clinical Research Center for Cancer/ Cancer Hospital, Chinese Academy of Medical Sciences and Peking Union Medical College, Beijing, People's Republic of China, Email zzx_20003@126.com

Background: Metastasis is a hallmark of cancer and the leading cause of cancer-related mortality. However, the mechanism underlying liver metastasis in colorectal cancer (CRC) remains incompletely understood. This study explores the role of long non-coding RNA (lncRNA) SLERT in promoting CRC liver metastasis by downregulating HUNK expression.

Methods: SLERT expression levels in CRC tissues were analyzed and correlated with patient survival outcomes. Functional assays, including migration and invasion assays, were performed to assess the impact of SLERT knockdown and overexpression on metastatic behavior. Mechanistic studies examined SLERT's interaction with the RNA-binding protein RBM15 and its effect on HUNK mRNA stability. The subcellular localization of SLERT was also determined.

Results: SLERT was significantly upregulated in CRC tissues and associated with poor survival outcomes. Silencing SLERT inhibited CRC cell migration and invasion, whereas its overexpression enhanced these metastatic properties. Mechanistically, SLERT interacted with RBM15, impairing its ability to stabilize HUNK mRNA, leading to decreased HUNK expression and increased metastatic potential. SLERT was primarily localized in the cytoplasm, indicating its active role in gene regulation within the tumor microenvironment.

Conclusion: LERT promotes liver metastasis in CRC by downregulating HUNK expression through RBM15-mediated mRNA destabilization. These findings suggest that SLERT could serve as a diagnostic biomarker and therapeutic target. Targeting SLERT or restoring HUNK expression may provide novel strategies to combat CRC liver metastasis and improve patient prognosis.

Keywords: CRC, liver metastasis, SLERT, HUNK, m6A

Introduction

Colorectal cancer (CRC) represents one of the most prevalent malignancies globally and remains a leading cause of cancer-related mortality.[1,2] It typically arises from adenomatous polyps in the colon or rectum, which possess the potential to progress into invasive carcinoma.[3] Among patients diagnosed with CRC, the liver is the predominant site of distant metastasis, with a considerable proportion developing liver metastases during the disease course.[4,5] Metastatic colorectal cancer (mCRC), particularly colorectal liver metastasis (CRLM), has a poor prognosis, with a 5-year survival rate of less than 20%.[6,7] CRLM is closely linked to tumor-induced angiogenesis, alterations in the tumor microenvironment, and immune evasion mechanisms.[8,9] The metastatic cascade is a complex, multistep process involving tumor cell invasion, intravasation, survival in circulation, extravasation, and subsequent colonization and proliferation within the hepatic parenchyma.[10] The presence of liver metastases, particularly in cases of rectal cancer, typically signifies advanced

Received: 19 January 2025
Accepted: 1 May 2025
Published: 9 May 2025

disease and is a critical determinant of patient prognosis.[11] Despite substantial advancements in the management of CRLM through enhanced surgical techniques, systemic chemotherapy, targeted therapies, and immunotherapeutic strategies, significant challenges persist, and overall survival outcomes remain suboptimal.[12–14]

Long non-coding RNA SLERT (lncSLERT) plays a key role in transcriptional regulation, particularly in RNA polymerase I-mediated rRNA synthesis.[15–17] Previous studies have suggested that SLERT is crucial for cell growth, differentiation, and stress response.[18,19] Abnormalities in the function or expression of SLERT may lead to cancer.[20] However, its role in CRC was unclear. Our study revealed that SLERT is overexpressed in CRC tissues compared to adjacent normal tissues. In vitro and in vivo functional experiments showed that SLERT gene knockdown could significantly inhibit the migration, invasion and liver metastasis of CRC cells, while SLERT overexpression had the opposite effect. In addition, mechanism exploration showed that SLERT competitively bound RBM15 inhibited the stabilizing effect of RBM15 on HUNK mRNA, reducing HUNK mRNA level, thereby enhancing the liver metastasis ability of colorectal cancer and changing the phenotype of CRC cells. In conclusion, our findings suggest that SLERT promotes colorectal cancer migration and invasion in the progression of colorectal cancer and promotes liver metastasis of colorectal cancer and outline the connection between lncSLERT and colorectal cancer, highlighting its potential roles in cancer progression, biomarker development.

Materials and Methods

Patients and Cohorts

We utilized 116 human colorectal cancer tissues and their corresponding adjacent non-cancerous tissues from the Cancer Hospital of the Chinese Academy of Medical Sciences in Beijing. The utilization of these clinical specimens was approved by the institutional research Ethics Committee, with written informed consent obtained from all patients. This study was conducted in accordance with the Declaration of Helsinki.

Cell Line and Cell Culture

Human normal colon epithelial cell line NCM460 and human colorectal cancer cell lines LoVo, SW480, SW620, HT-29, HCT116 were purchased from the Chinese Academy of Sciences cell bank. All cell lines used in our study were validated by STR analysis. Lovo cells were cultured in Ham's F-12K (Gibco). HCT116 was cultured in Dulbecco's Modified Eagle Medium (Gibco). The cells were cultured with 1% penicillin-streptomycin double antibody supplemented with 10% heat-inactivated fetal bovine serum at 37°C and 5% CO2.

Plasmid Construction

The lentiviral vector TetIIP-TurboRFP-MCS(MIR30)-Ubi-TetR-IRES-Puromycin containing the SLERT short hairpin RNA (shSLERT) and shRNA scramble (shNC) was provided by Shanghai Genechem Co.,Ltd. The shSLERT sequence and shNC sequence can be found in Table S1. Small interfering RNAs (siRNAs) and corresponding negative control siRNA scramble (si-NC) used in the study were purchased from Wuhan JinTuoSi Biotechnology Co., Ltd. The sequences of siRNA for KD used are listed in Table S2. To overexpress SLERT and HUNK, the full-length sequence was synthesized and inserted into pLVX-Puro vector.

Lentivirus Packaging and Generation of Stable Cell Lines

Lentiviruses were produced by co-transfection of 293T cells with a specific shRNA Vector or pLVX-SLERT, and packaging vectors psPAX2 and pMD2.G, using X-tremeGENE HP DNA transfection reagent (Roche, Switzerland). The virus was harvested and filtered at 48h and 72h after transfection. To establish stable cell lines, CRC cells were in fected using lentiviral supernatant for 24 h and then maintained with fresh complete medium containing 2μg/mL puromycin for a continuous 2-week period.

Quantitative Real-Time PCR, qRT-PCR

The total RNA of tissue samples and cells was extracted by TRIzol reagent (Invitrogen, CA, USA), The RNA separation from the nuclear and cytosolic fractions of LoVo and HCT116 cells was purified using the Ambion™ PARIS™ Kit

(AM1921, Invitrogen, CA, USA), following the manufacturer's instructions, and cDNA was synthesized by Reverse Transcriptase M-MLV (RNase H-) (2641Q, Takara, Japan). Then, gene amplification and quantification were tested by Hieff qPCR SYBR Green Master (11199ES25, Yeasen, Shanghai, China) with the QSDX-1 Real time PCR (ABI, USA). Based on qPCR results, the relative expression levels of SLERT and HUNK mRNA in tissue samples or cells were calculated by 2-ΔΔCT using GAPDH, U6 or S18 as internal reference genes. Primer sequences are provided in Table S3.

Western Blotting

Cells were disrupted using a sufficient volume of RIPA lysis buffer (BL504A; Biosharp, Hefei, China) augmented with protease inhibitor and Phosphatase inhibitor on ice for 20 minutes, succeeded by centrifugation at 13,000×g for 30 minutes at 4 °C to acquire a translucent protein supernatant. The protein concentration was quantified with a BCA protein assay kit (23225, Thermo Fisher Scientific, Waltham, MA, USA). Identical amounts of protein were loaded onto 10% (wt/vol) sodium dodecyl sulfate polyacrylamide gels (SDS-PAGE), segregated by electrophoresis, and subsequently transferred onto polyvinylidene fluoride (PVDF) membranes (Millipore Corporation, Billerica, MA, USA). The membranes were blocked with 5% BSA at room temperature for 1 hour, followed by an overnight incubation with primary antibodies at 4 °C. After undergoing four washes with TBST for 10 minutes each, the membranes were treated with secondary antibodies conjugated to a fluorescent tag (Invitrogen) at room temperature for 2 hours and subsequently rewashed with TBST. Detection of all membranes was executed using an enhanced chemiluminescent substrate kit (34095, Thermo Fisher Scientific) and an Odyssey Infrared Imaging System (LI-COR, USA). Antibody information is provided in Table S4.

CCK-8 Assays

The impact of varying SLERT expression levels on cell proliferation activity was assessed using the CCK8 assay. LoVo and HCT116 cells, either stably low-expressing or overexpressed, were digested with pancreatic enzymes and subsequently inoculated 1,000 cells per well into 96-well plates for incubation at 37°C in a 5% CO_2 atmosphere. After incubation periods of 24 hours, 48 hours, 36 hours, and 72 hours, the culture medium was removed, and 10 μL of CCK8 solution (MA0218, Meilunbio, Dalian, China) was added to each well for an additional incubation period of 2 hours. Finally, the absorbance at 450 nm for each well was measured using an enzyme-labeled instrument.

Clone Formation Assay

A total of LoVo and HCT116 cells were seeded into a six-well plate (1000 cells per well) and subsequently cultured. The cells were incubated at 37°C in a humidified atmosphere containing 5% CO_2 for 8–10 days. Following incubation, the colonies were fixed with formalin for 30 minutes and then stained with 0.1% crystal violet for 15 minutes. Finally, photographs and counts were taken of colonies containing at least 50 cells.

Wound Healing Assay

Cell migration was detected by scratch assay: LoVo or HCT116 cells were inoculated in the pore. After overnight culture, scratches were made on the cell layer perpendicular to the cell plane, and the non-adherent cells were washed away with PBS. The fresh culture medium without serum was replaced and cultured in an incubator at 37 °C and 5%CO2. The scratch distance was observed and photographed with a microscope at 0 h and 24 h, respectively.

Transwell Assay

The cell migration and invasion were tested using 24-well Transwell plates. 2×10^4 LoVo and 2×10^4 HCT116 cells were collected by covering the Transwell chamber with matrix glue as needed, and the cells were re-suspended using serum-free medium. Cell suspension was added to the upper chamber of Transwell, and culture medium containing serum was added to the 24-well plate of the lower chamber. After 48 h of culture, cells invading the lower surface of the upper chamber were fixed with methanol and stained with crystal violet. Finally, the number of cells invading in 5 visual field areas was randomly counted under the microscope.

Dual-Luciferase Reporter Assay

LoVo and HCT116 cells were transfected with the pcDNA3.1-SLERT plasmid and pGL3-basic plasmids containing full-length and mutated DNA sequences, constructed using the Ready-to-Use Seamless Cloning Kit (Sangon). After transfection with Lipofectamine 3000, cells were seeded in 24-well plates and co-transfected with pGL3-Basic-HUNK. Following a 48-hour incubation, the dual-luciferase reporter assay was conducted using the Dual-Luciferase Reporter Assay System (Promega) according to the manufacturer's guidelines to assess the effect of SLERT on HUNK transcriptional activity.

mRNA-Seq

Total mRNA was isolated from CRC cells with the TRIzol reagent (Thermo Fisher). After quality control, three random control samples and three experimental samples underwent sequencing with the Illumina HiSeq 4000 platform (LC-Bio Technologies, Hangzhou, China).Genes with differential expression are defined as those with a fold change ≥ 1 and a p-value ≤ 0.05. The data analysis was conducted by Beijing Annoroad Gene Technology Corp., Ltd.

RNA Binding Protein Immunoprecipitation (RIP)-qPCR

The RIP procedure is conducted using the Magana RIP Quad Kit (Millipore) to identify m6A modifications or RNA-binding proteins associated with a specific gene, following the guidelines provided by the manufacturer. In this process, $1.0 \times 10\text{^}7$ cells are subjected to treatment with 200 μL of RIP lysis buffer; from this, 15 μL of supernatant is reserved as input while 150 μL of supernatant enriched with antibody or rabbit IgG linked to protein A/G magnetic beads in IP buffer containing RNase inhibitor is incubated overnight at 4°C. After washing steps, the immunoprecipitated RNA undergoes digestion, purification, and subsequent analysis via qPCR.

In vivo Experiments

All animal procedures were approved by the Institutional Animal Care and Use Committee (IACUC) at the Cancer Hospital of the Chinese Academy of Medical Sciences and were conducted in accordance with the Guidelines for the Care and Use of Laboratory Animals issued by the National Institutes of Health (NIH). 6-week-old female BALB/c-nu mice were procured from BEIJING HFK BIOSCIECE CO.,LTD. For spleen injections, weigh the mouse and administer anesthesia via intraperitoneal injection using Avertin at a dosage ranging from 125μg to 250μg per gram of body weight. Position the mouse on its left side, expose the splenic area, and disinfect the skin covering the spleen with 75% alcohol. Make a horizontal incision of approximately 1cm in length on the skin, located roughly 1–2cm below the left chest ribs. Carefully cut through both the skin layer and the underlying muscle layer. Gently clamp the fat adhered to the spleen and pull it out along with the spleen itself. Utilize an insulin syringe to inject $5\times10\text{^}6$ hCT116 cells, resuspended in 50 μL of PBS, into the distal tissue of the spleen. Apply gentle pressure to the spleen with a cotton swab for approximately 15 minutes to ensure cellular absorption. Subsequently, ligate the splenic artery and vein using absorbable sutures, separate the spleen, and excise it. Close the incision with absorbable surgical sutures to prevent any bleeding. Throughout the duration of the experiment, the animal is continuously monitored until it passes naturally or is euthanized (over a period of 30 days). Real-time imaging assessments are performed to evaluate liver metastases.

Statistical Analysis

All experiments were carried out no less than three times, and the results were depicted as means ± SD. The Student's *t*-test and one-way analysis of variance (ANOVA) were adopted to analyze the data, while chi-square tests were exploited to assess categorical variables. All statistical examinations were implemented using SPSS 16.0 (SPSS, Chicago, IL, USA), and p values < 0.05 were regarded as denoting statistically significant differences ($^*p < 0.05$, $^{**}p < 0.01$, $^{***}p < 0.001$).

Results

SLERT Is Upregulated in CRC and Its High Expression Is Associated with Poor Prognosis

We evaluated SLERT expression in 116 colorectal carcinoma (CRC) patients using RNA fluorescence in situ hybridization (RNA-FISH). Notably, CRC tissues exhibit a significantly higher expression of SLERT, as indicated by a distinct red fluorescence signal (Figure 1A and B). The diagnostic potential of SLERT was further supported by a receiver operating characteristic (ROC) curve, which revealed a decent ability to differentiate CRC from normal tissues, with an Area Under the Curve (AUC) of 0.802 (Figure 1C). Furthermore, correlation analyses between SLERT expression and clinicopathologic features showed significant associations. Patients with high SLERT expression were older (p=0.022), had more advanced tumor infiltration stages (T3+T4, p=0.023), had a higher occurrence of lymph node metastasis (p=0.018), and were more likely to be in advanced TNM stages (III+IV, p=0.049) (Table 1). Moreover, Kaplan-Meier survival analysis emphasizes that an elevated SLERT expression is associated with markedly poorer overall survival in CRC patients ($P = 0.025$), reinforcing its prognostic significance (Figure 1D). We also compared SLERT expression in CRC tissues using qRT-PCR, normalizing to GAPDH expression. The results demonstrated that SLERT expression was significantly higher in CRC tissues compared to normal tissues ($P < 0.01$) (Figure 1E). This upregulation was observed in various CRC cell lines (LoVo, SW480, SW620, HT-29, HCT116) relative to the normal colon epithelial cell line NCM460 (Figure 1F). To further define SLERT's cellular localization in CRC cells, we performed qRT-PCR, which confirmed that SLERT is predominantly localized in the cytoplasm rather than the nucleus in both LoVo and HCT116 cells (Figure 1G). This finding is supported by RNA-FISH (Figure 1H). Quantitative evaluations of SLERT localization reveal a higher cytoplasmic-to-nuclear ratio in both cell lines (Figure 1I). Collectively, these findings imply that SLERT is not only upregulated in CRC tissues and cell lines but also primarily situated in the cytoplasm, with its increased expression linked to adverse prognostic outcomes in CRC patients.

SLERT Promotes the Migration and Invasion of Colorectal Cancer in vitro

To investigate the role of SLERT in colorectal cancer cell functions, we used lentiviral vectors to generate LoVo and HCT116 cell lines with stable knockdown or overexpression of SLERT (Figure S1A and S1B). Through CCK8 and colony formation assays, we found that SLERT overexpression had no significant effect on cell proliferation or colony formation in either cell line compared to the control group (Figure 2A, B and S1C). Similarly, knockdown of SLERT using two distinct shRNAs showed no significant impact on proliferation or colony formation compared to the negative control (Figure 2C, D and S1D). However, using a Transwell chamber assay to assess cell migration and invasion, we observed that SLERT overexpression significantly increased migration and invasion in both LoVo and HCT116 cells. In contrast, SLERT knockdown notably reduced these capabilities, as reflected by the decreased number of migrating and invading cells (Figure 2E and F). Additionally, the wound healing assay demonstrated that SLERT overexpression enhanced the migration rate, while SLERT knockdown diminished it compared to the control group (Figure 2G and H). These findings suggest that, while SLERT modulation does not affect cell proliferation or colony formation, it plays a significant role in promoting cell migration and invasion, indicating its involvement in colorectal cancer cell motility and invasiveness. Therefore, altering SLERT expression may influence the metastatic potential of colorectal cancer cells.

SLERT Promotes CRC Liver Metastasis in vivo

Given that SLERT significantly enhances the migration and invasion capacity of colorectal cancer cells in vitro, while SLERT knockdown inhibits these capabilities, we further investigated its role in colorectal cancer metastasis in vivo, focusing particularly on liver metastasis. To this end, we developed an in vivo colorectal liver metastasis (CRLM) model by injecting luciferase-labeled human colorectal cancer cells into the spleens of BALB/c nude mice. Using an in vivo imaging system (IVIS), we assessed liver metastatic load and observed that SLERT overexpression in HCT116 cells significantly promoted liver metastasis. This was evident from the higher fluorescence intensity in the liver region of the SLERT overexpression group compared to the control group (Figure 3A). Whole-liver images and hematoxylin and eosin (H&E) staining further confirmed the presence of more prominent liver metastases in the SLERT group (Figure 3B).

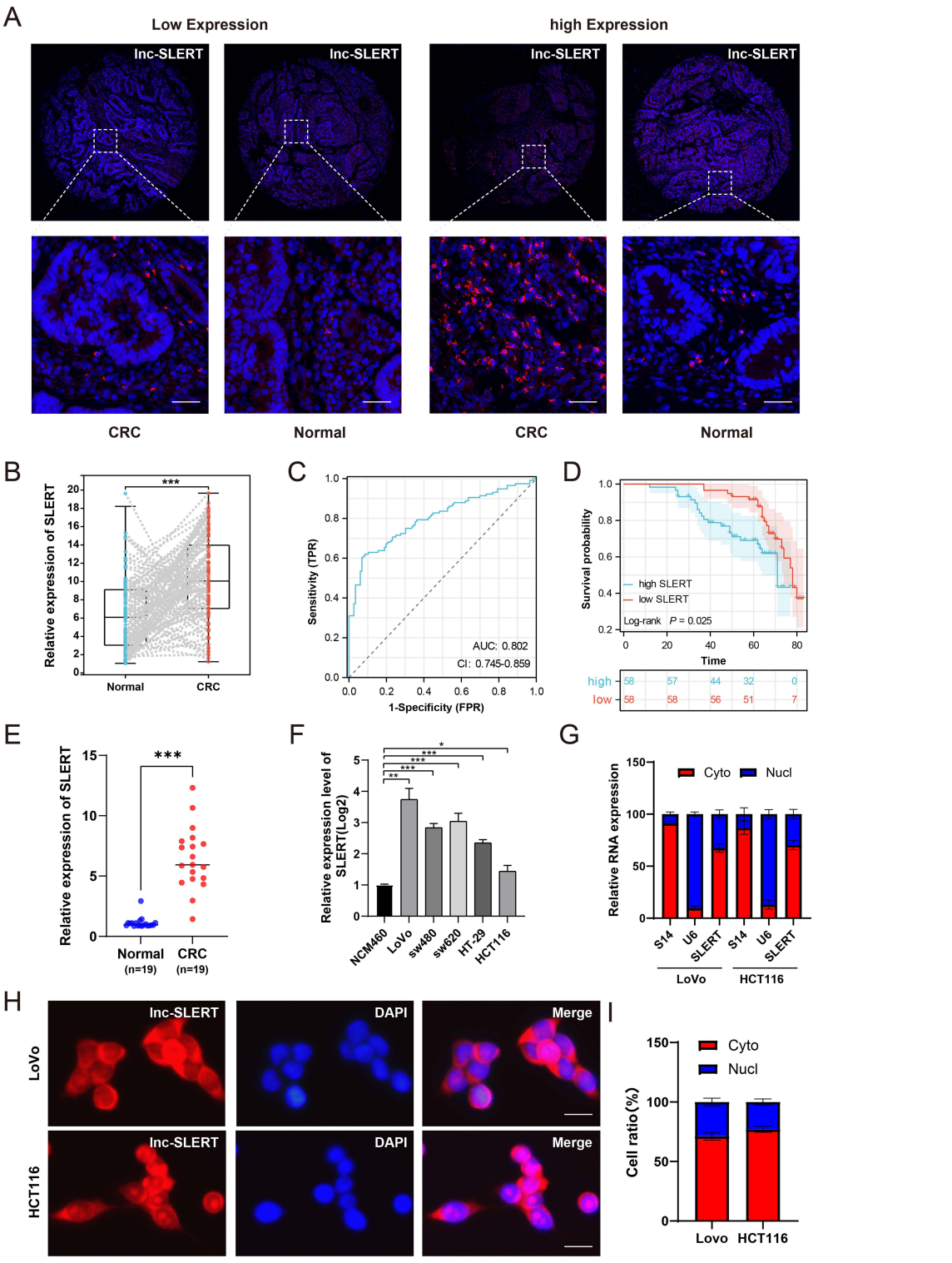

Figure 1 SLERT is upregulated in CRC and its high expression is associated with poor prognosis. (**A**) RNA fluorescence in situ hybridization (RNA-FISH) images illustrating SLERT expression in CRC and normal tissues, with red fluorescence indicating SLERT and blue fluorescence indicating DAPI. Scale bar: 50 μm. (**B**) Quantification of SLERT expression in CRC and normal tissues based on RNA-FISH analysis. ***P < 0.001. (**C**)Receiver operating characteristic (ROC) curve analysis to assess SLERT's diagnostic potential in CRC. (**D**) Kaplan-Meier survival curve analysis of SLERT expression in relation to overall survival in CRC patients (P = 0.025). Data calculated from a Log rank test. (**E**) Quantification of SLERT expression in CRC and normal tissues using qRT-PCR. ***P < 0.001. (**F**) Assessment of SLERT expression in CRC cell lines (LoVo, SW480, SW620, HT-29, HCT116) compared to the normal colon epithelial cell line NCM460 via qRT-PCR. *P < 0.05, **P < 0.01, ***P < 0.001. (**G**) qRT-PCR analysis was conducted to determine the localization of SLERT in LoVo and HCT116 cells. S18 and U6 were respectively utilized as cytoplasmic and nuclear markers. (**H**) RNA-FISH images of SLERT in LoVo and HCT116 cells, confirming its cytoplasmic localization. Scale bar: 100 μm. (**I**) Quantitative analysis of the cytoplasmic-to-nuclear ratio of SLERT in LoVo and HCT116 cells.

 https://doi.org/10.2147/OTT.S514001

Table 1 Correlation Between SLERT Expression and Clinicopathologic Features (N = 116)

Clinicopathologic Features	All Patients	Expression of SLERT		p-value
		Low (n = 58)	High (n = 58)	
Gender				NS
Female	52(44.8%)	29	23	
Male	64(55.2%)	29	35	
Age, years				0.022
<60	45(38.8%)	29	16	
≥60	71(61.2%)	29	42	
Tumour size, cm				NS
<5	65(56.0%)	30	35	
≥5	51(44%)	28	23	
Tumour infiltration				0.023
T1 + T2	25(21.6%)	7	18	
T3 + T4	91(78.4%)	51	40	
Lymph node metastasis				0.018
No	77(66.4%)	45	32	
Yes	39(33.6%)	13	26	
Distant metastasis				NS
No	110(94.8%)	56	54	
Yes	6(5.2%)	2	4	
TNM stage				0.049
I + II	77(66.4%)	44	33	
III + IV	39(33.6%)	14	25	

Additionally, the SLERT overexpression group showed a significant increase in liver weight and the percentage of liver metastases compared to the vector control group (Figure 3C). Conversely, knockdown of SLERT in HCT116 cells markedly reduced liver metastasis, as indicated by lower fluorescence intensity in the liver region compared to the control group (Figure 3D). Whole-liver images and H&E staining in the SLERT knockdown groups demonstrated a clear reduction in liver metastasis relative to the shCtrl group (Figure 3E). Both shSLERT-1 and shSLERT-2 groups exhibited significantly lower liver weights and a reduced percentage of liver metastases compared to the control group (Figure 3F).

SLERT Reduces the Expression of HUNK in CRC Cells

We investigated the role of SLERT in regulating downstream targets associated with the biological behavior of colorectal cancer liver metastasis by manipulating SLERT expression in CRC cells. Specifically, SLERT was knocked down in LoVo cells and overexpressed in HCT116 cells. RNA sequencing conducted after these manipulations revealed hormone-regulated neurogenic kinase (HUNK), an 80 kDa protein, as a key downstream target of SLERT. The volcano plots demonstrated the differentially expressed genes in LoVo and HCT116 cells after SLERT manipulation. Notably, HUNK was significantly downregulated in HCT116 cells and upregulated in LoVo cells, underscoring its association with SLERT expression (Figure 4A). The bubble chart visualized the top 10 enriched KEGG pathways linked to the SLERT, with a particular focus on the PI3K-Akt and MAPK signaling pathways. The size of the bubbles represented the number of genes involved, while their color indicated the significance of pathway enrichment (Figure 4B). Additionally, a Venn diagram illustrated the overlap of upregulated and downregulated genes between LoVo and HCT116 cells, showing that HUNK was among the genes upregulated in LoVo cells following SLERT knockdown, while it was downregulated in HCT116 cells upon SLERT overexpression (Figure 4C). To validate these findings, we performed qPCR to assess the relative mRNA levels of SLERT and HUNK under different conditions. The results confirmed that SLERT knockdown in LoVo cells led to increased HUNK

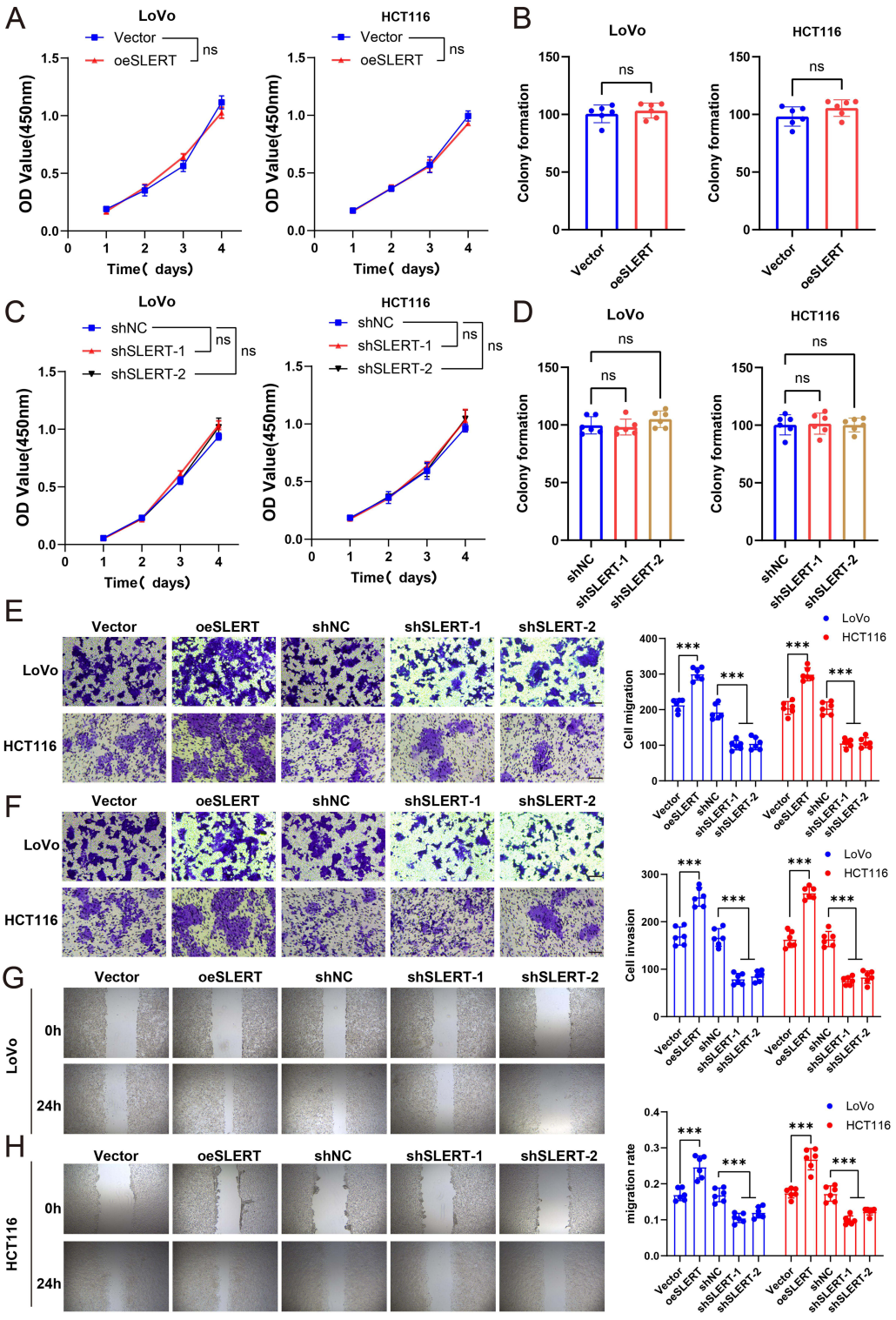

Figure 2 SLERT promotes the migration and invasion of colorectal cancer in vitro. (**A**) CCK8 assay in LoVo and HCT116 cells over 4 days, comparing cell proliferation after SLERT overexpression with corresponding controls. ns: no significance. (**B**) Colony formation assay in LoVo and HCT116 cells, evaluating colony-forming ability following SLERT overexpression or knockdown, compared to controls. ns: no significance. (**C**) CCK8 assay in LoVo and HCT116 cells over 4 days, comparing cell proliferation after knockdown with corresponding controls. ns: no significance. (**D**) Colony formation assay in LoVo and HCT116 cells, evaluating colony-forming ability following knockdown, compared to controls. ns: no significance. (**E**) Transwell assays without matrigel were used to evaluate the migration ability of LoVo (upper) and HCT116 (lower) cells after SLERT knockdown or overexpression, with quantitative analysis shown on the right. Scale bar: 1000 μm. ***P < 0.001. (**F**) Transwell invasion assay with matrigel in LoVo (upper) and HCT116 (lower) cells, measuring invasion after SLERT overexpression or knockdown, with quantitative analysis shown on the right. Scale bar: 100 μm. ***P < 0.001. (**G** and **H**) Wound healing assay in LoVo and HCT116 cells at 0 and 24 hours, evaluating migration post-transfection with SLERT overexpression or knockdown. Quantitative analysis of migration and invasion is shown alongside the respective panels. Scale bar: 500 μm. ***P < 0.001.

https://doi.org/10.2147/OTT.S514001

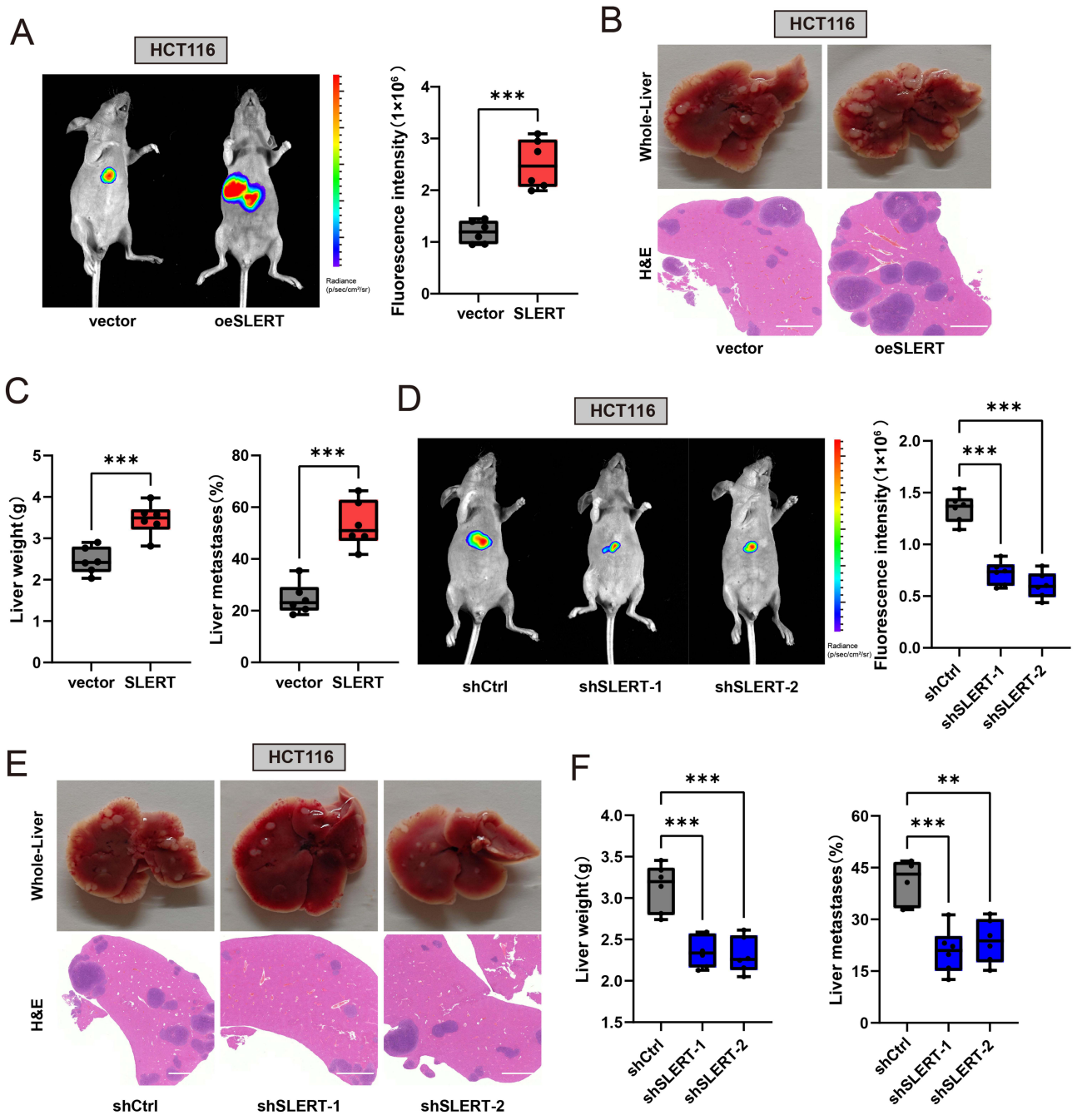

Figure 3 SLERT promotes colorectal cancer liver metastasis in vivo. **(A)** Cells overexpressing SLERT and scrambled cells were injected into the spleens of BALB/c nude mice. IVIS imaging was conducted on HCT116 cells with SLERT overexpression to assess fluorescence intensity in the liver, thereby evaluating metastasis (n = 6). ***P < 0.001. (**B**) Representative gross specimens (upper) and HE staining (lower) of metastatic lesions in the liver from both SLERT overexpression and control groups. Scale bar: 500 μm. (**C**) Comparison of liver weight and metastasis percentage between SLERT overexpression and control groups. ***P < 0.001. (**D**) IVIS imaging after SLERT knockdown in HCT116 cells, with fluorescence intensity indicating liver metastasis (n = 6). ***P < 0.001. (**E**) Whole-liver images and H&E staining to assess liver metastasis in the shSLERT-1, shSLERT-2, and control groups. Scale bar: 500 μm. (**F**) Evaluation of liver weight and metastasis percentage in the SLERT knockdown groups compared to the control. **P < 0.01, ***P < 0.001.

expression, while SLERT overexpression in HCT116 cells resulted in decreased HUNK expression (Figure 4D and E). Western blot analysis further confirmed these results, showing protein levels of HUNK across the different conditions. HUNK expression was reduced in HCT116 cells with SLERT overexpression and increased in LoVo cells with SLERT knockdown, in line with the mRNA expression results (Figure 4F). Overall, these findings suggest that SLERT negatively

https://doi.org/10.2147/OTT.S514001

regulates HUNK expression at both the mRNA and protein levels in colorectal cancer cells, and that modulation of SLERT impacts key oncogenic pathways such as the PI3K-Akt and MAPK pathways.

SLERT Influences m6A Modification and HUNK Expression, Through Interaction with RBM15

Upon validation via RNA sequencing and experimental verification that SLERT knockdown or overexpression can markedly modulate HUNK expression, we delved further into the underlying regulatory mechanism. The relative luciferase activity was measured in LoVo and HCT116 cell lines transfected with a negative control or two different shSLERT knockdowns. No significant differences were observed between the groups, indicating that SLERT knockdown did not affect luciferase activity (Figure 5A). Similarly, when these cell lines were transfected with either a control vector or SLERT at different concentrations (3 μg and 5 μg), no significant differences in luciferase activity were observed,

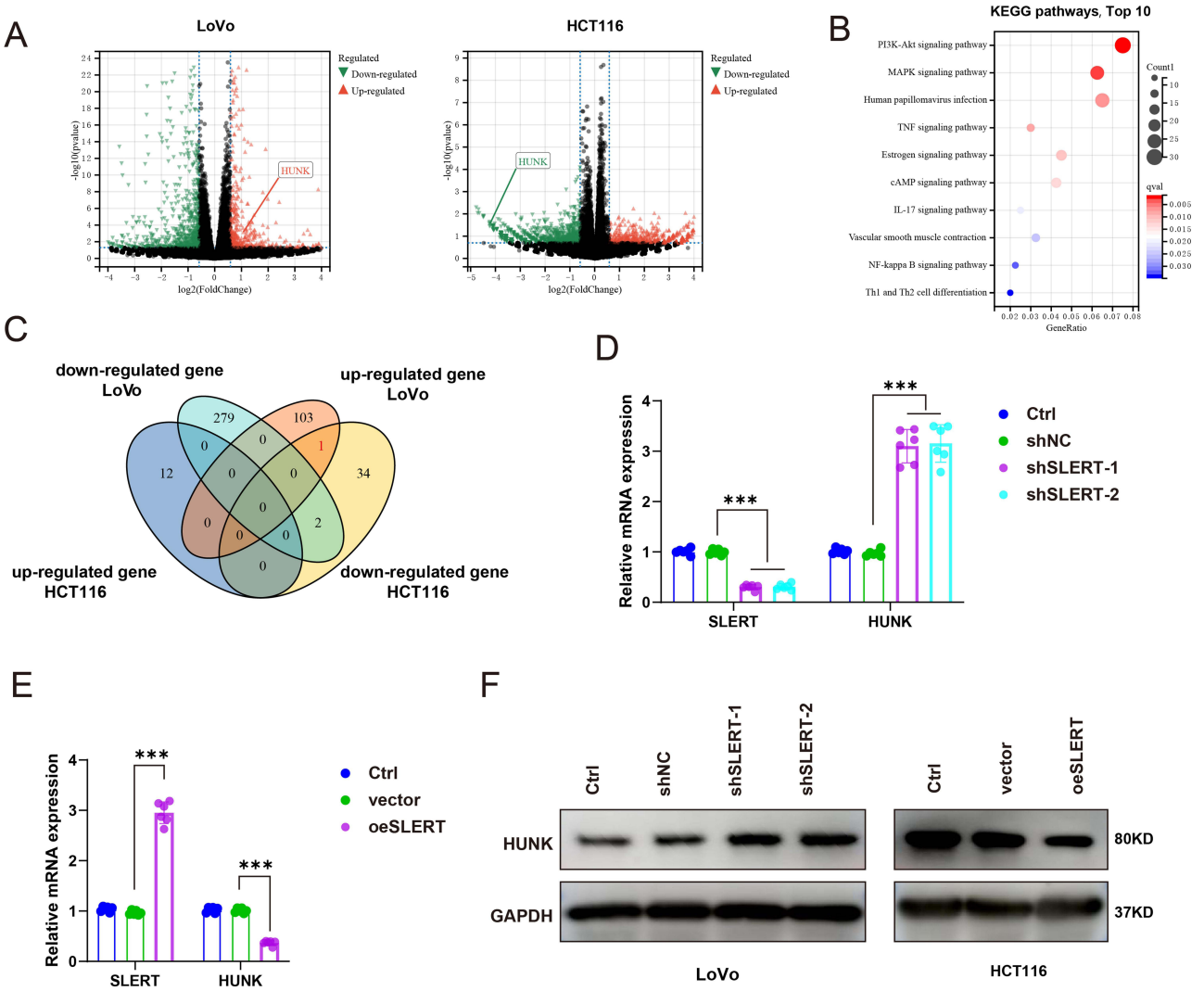

Figure 4 SLERT reduces the expression of HUNK in CRC cells. (**A**)Volcano plots showing differentially expressed genes in LoVo (left) and HCT116 (right) cells after SLERT knockdown and overexpression, respectively. Red triangles indicate upregulated genes, and green triangles represent downregulated genes. (**B**) Bubble chart depicting enriched pathways related to differentially expressed genes, highlighting PI3K-Akt and MAPK signaling pathways. The bubble size reflects the number of genes involved, and the color gradient represents enrichment significance (q-value). (**C**) Venn diagram illustrating the overlap of upregulated and downregulated genes in LoVo and HCT116 cells after SLERT manipulation. HUNK appears as an upregulated gene in LoVo cells and a downregulated gene in HCT116 cells. The red font highlights the intersection of genes that were selected in our study. (**D** and **E**) qRT-PCR analysis of SLERT and HUNK mRNA levels. SLERT knockdown in LoVo cells (**D**) led to an increase in HUNK expression, while SLERT overexpression in HCT116 cells (**E**) resulted in decreased HUNK expression. Data are presented as mean ± SD, ***p < 0.001. (**F**) expression in LoVo cells after SLERT knockdown and decreased HUNK expression in HCT116 cells after SLERT overexpression. GAPDH was used as a loading control.

 https://doi.org/10.2147/OTT.S514001

further suggesting that SLERT does not influence the transcriptional activity of HUNK (Figure 5B). Since variations in HUNK expression may entail epigenetic modulation, we concentrated on whether SLERT governs HUNK expression by influencing m6A RNA modification, a significant epigenetic modification. The expression levels of m6A-related genes (CBLL1, RBM15, VIRMA, ALKBH5, RBMX, YTHDF1) were compared among three groups: G1 (HUNK low), G2 (HUNK high), and Normal. Significant differences were observed across all genes with highly significant p-values, indicating increased expression in G1 and G2 groups compared to the Normal group (Figure 5C). The relative m6A levels of HUNK were assessed in LoVo and HCT116 cell lines with shNC and two different shSLERT knockdowns. A significant increase in m6A levels was observed in both cell lines with SLERT knockdown compared to the shNC control (Figure 5D). Conversely, in cells transfected with SLERT at concentrations of 3 μg and 5 μg, a significant decrease in m6A levels was observed compared to the vector control (Figure 5E). Specifically, considering that RBM15 is a key modulator of m6A modification, we further scrutinized the interaction between SLERT and RBM15 to explore whether this interaction assumes a pivotal role in the regulation of HUNK expression. SLERT knockdown significantly increased HUNK expression compared to the vector, and this effect was reversed when RBM15 was also disturbed (Figure 5F). Finally, an RNA pull-down assay confirmed that RBM15 was strongly enriched by the SLERT probe (Figure 5G), and similarly, SLERT was also pulled down using an RBM15 antibody (Figure S2A and S2B).

SLERT Promotes Liver Metastasis in Colorectal Cancer by Regulating HUNK and the PI3K/AKT Pathway

Western blot analysis revealed that SLERT knockdown in LoVo and HCT116 colorectal cancer cells significantly reduced the levels of phosphorylated PI3K and phosphorylated AKT, indicating its involvement in the PI3K/AKT signaling pathway. Interestingly, when SLERT knockdown was combined with HUNK intervention, the levels of phosphorylated PI3K and phosphorylated AKT increased, suggesting that SLERT regulates this signaling pathway through HUNK (Figure 6A, S3A and S3B). In vivo imaging of mice demonstrated that SLERT overexpression markedly enhanced fluorescence intensity, indicating a higher metastatic tumor burden in the liver. While SLERT overexpression promoted liver metastasis, co-overexpression of HUNK mitigated this effect, suggesting that SLERT's role in promoting metastasis is modulated by HUNK (Figure 6B and C). Histological HE staining analysis corroborated these findings, showing more extensive liver metastasis with SLERT overexpression, while HUNK overexpression diminished both the metastatic spread (Figure 6D). Further analysis of mouse liver samples indicated that SLERT overexpression augmented the number of metastatic nodules, liver metastasis, and overall liver weight. Nevertheless, these effects were significantly alleviated when HUNK was concurrently overexpressed (Figure 6E and F). A schematic diagram outlines the proposed mechanism by which SLERT promotes liver metastasis in colorectal cancer: SLERT competes with RBM15, inhibiting its stabilizing effect on HUNK mRNA, leading to decreased HUNK expression and thereby facilitating liver metastasis (Figure 6G).

Discussion

Our study underscored the pivotal role of long non-coding RNA (lncRNA) SLERT in the progression of colorectal cancer (CRC), particularly through its down-regulation of HUNK expression, which facilitated liver metastasis. We observed significantly elevated levels of lncSLERT in CRC tissues, and its correlation with poor prognosis suggested that lncSLERT served as a promising biomarker for clinicians to stratify patients based on metastatic risk assessment. Furthermore, SLERT impeded its stabilizing effect on HUNK mRNA via competitive binding to RBM15, unveiling a novel regulatory axis with significant implications for colorectal cancer progression. The HUNK gene was implicated in various cellular processes, including apoptosis and cell cycle regulation; thus, its down regulation contributed to increased aggressiveness of CRC cells.[21,22] This finding indicated that SLERT not only influenced the behavior of cancer cells but also functioned as a broader regulator within the tumor microenvironment. Importantly, SLERT's involvement in modulating m6A modifications added another layer of complexity to its functionality. Given that m6A modifications were known to impact mRNA stability, translation efficiency, and splicing dynamics, SLERT's capacity to regulate these processes could yield new insights into how lncRNAs shaped the evolving landscape of cancer biology.[23–25] Our study further emphasized the necessity to investigate lncRNAs within the context of the tumor microenvironment. The

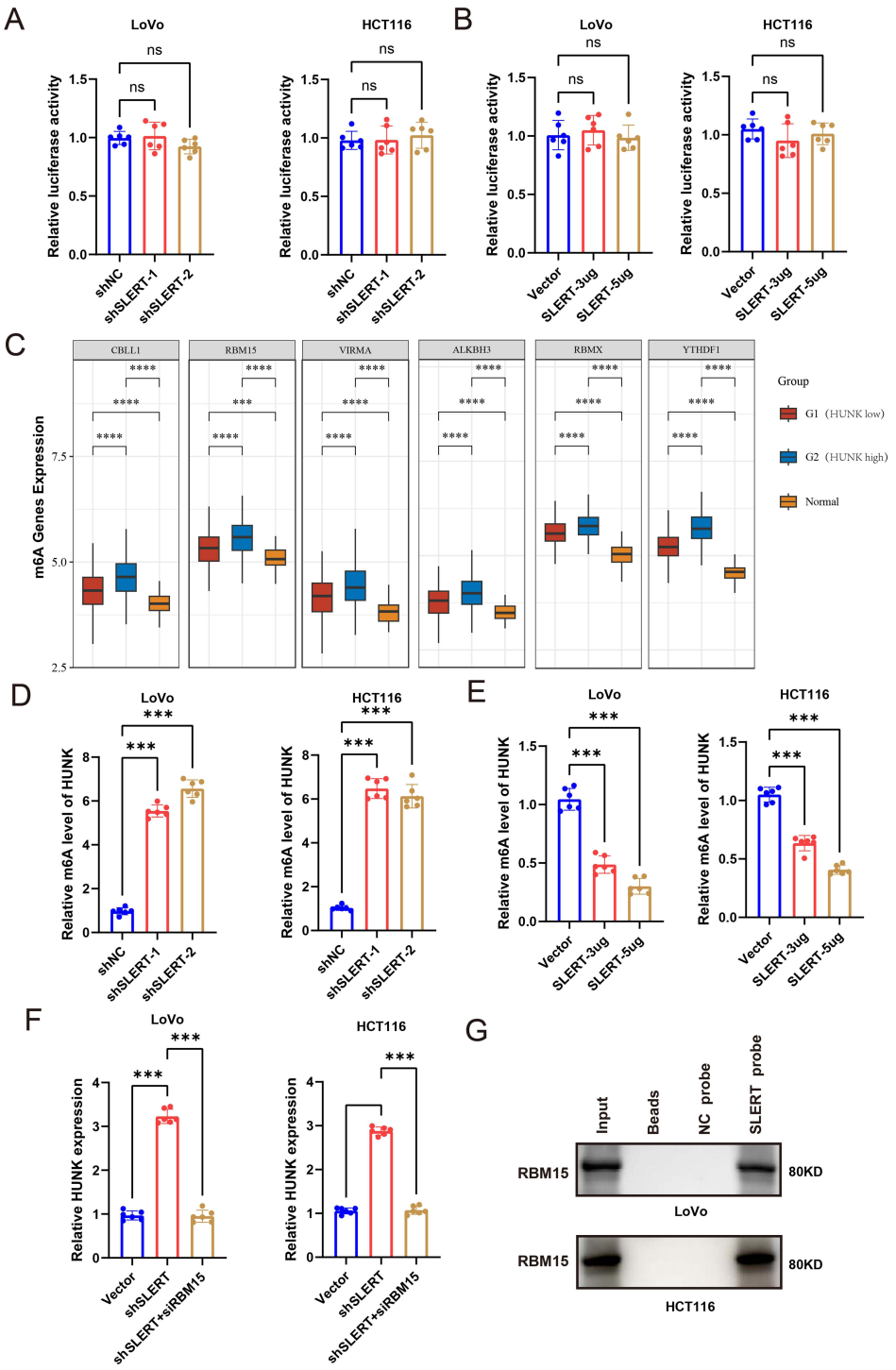

Figure 5 SLERT influences m6A modification and HUNK expression through interaction with RBM15. (**A** and **B**) Measurement of relative luciferase activity in LoVo and HCT116 cells following SLERT knockdown (**A**) and SLERT overexpression (**B**). Data represent the luciferase activity normalized to a control vector. Statistical analysis was performed to evaluate differences between groups, indicating no significant differences among the conditions. (**C**) This distribution diagram presents the expression levels of m6A-related genes in tumor versus normal tissues, utilizing publicly available data from the TCGA database. The horizontal axis represents different m6A-related genes, while the vertical axis displays their expression distributions. Box plots illustrate the expression levels of genes such as CBLL1, RBM15, VIRMA, ALKBH5, RBMX, and YTHDF1, categorized into three groups: G1 (HUNK low), G2 (HUNK high), and Normal. The significance of three groups of samples is tested by the Kruskal–Wallis test. ***P < 0.001, ****p < 0.0001. (**D** and **E**) Quantification of relative m6A levels of HUNK in LoVo and HCT116 cells following SLERT knockdown (**D**) and overexpression (**E**). m6A levels were measured using RIP assays. ***p < 0.001. (**F**) Relative expression of HUNK in LoVo and HCT116 cells assessed via qRT-PCR. The effect of SLERT knockdown on HUNK expression was measured, and the potential reversal of this effect by simultaneous knockdown of RBM15 was also analyzed. ***p < 0.001. (**G**) RNA pull-down assay demonstrating the enrichment of RBM15 using the SLERT probe in both LoVo and HCT116 cells. This assay confirms a direct interaction between SLERT and RBM15, indicating the specificity of the binding.

Abbreviation: ns, no significance.

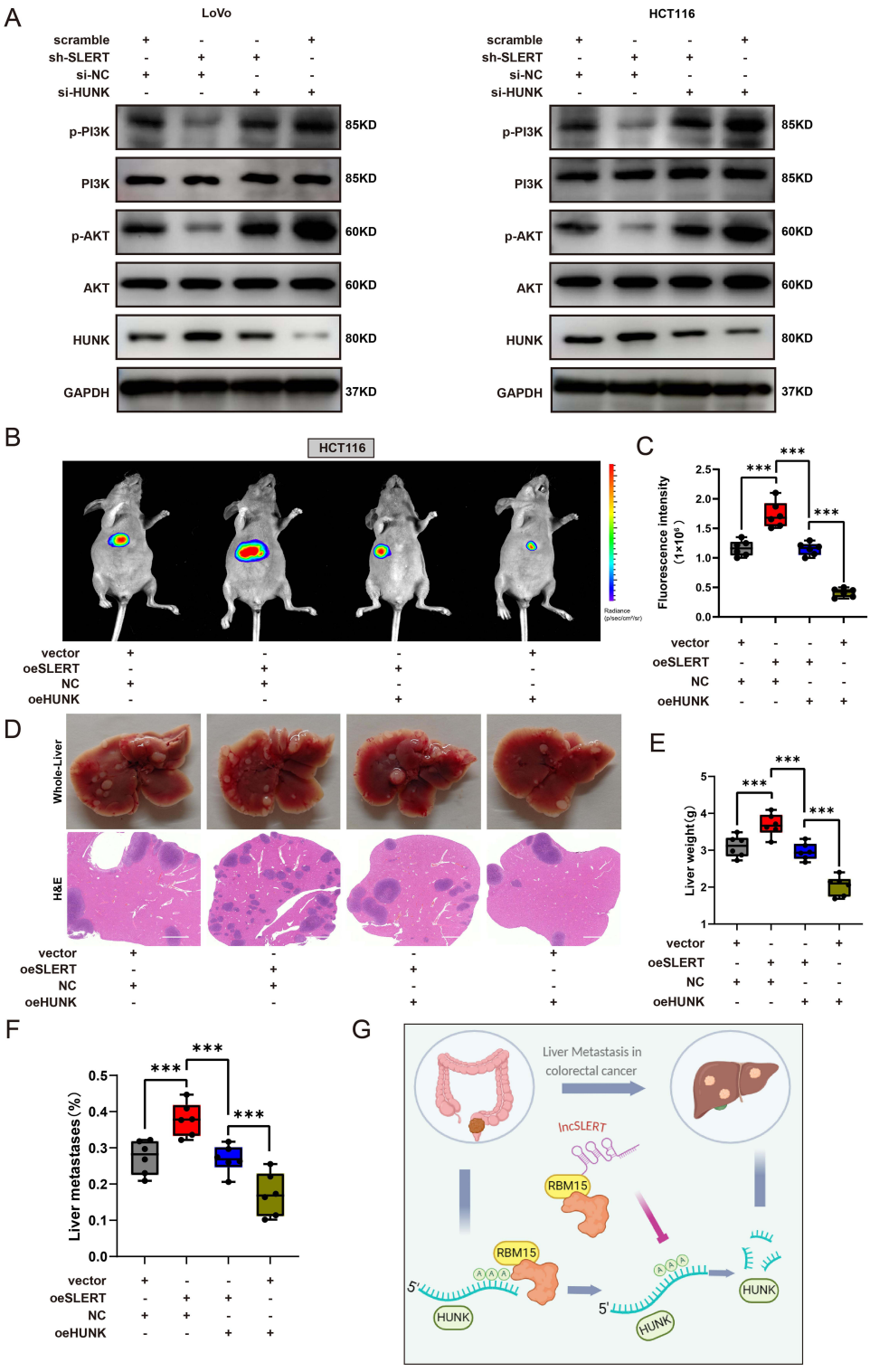

Figure 6 SLERT promotes liver metastasis in colorectal cancer by regulating HUNK and the PI3K/AKT pathway. (**A**) Western blot analysis was conducted to assess the expression of HUNK and the phosphorylation status of its downstream signaling pathway in SLERT knockdown LoVo cells (left) and HCT116 cells (right), both with and without HUNK knockdown. The silencing of HUNK expression partially mitigated the effects induced by SLERT knockdown. (**B**) In vivo imaging of liver metastases in mice injected with HCT116 cells, assessing fluorescence intensity to evaluate metastatic burden following SLERT overexpression. (**C**) Quantification of fluorescence intensity from in vivo imaging to analyze the impact of SLERT and HUNK expression on metastasis. ***$p < 0.001$. (**D**) Whole liver and histological analysis (HE staining) of liver metastasis, examining metastatic nodule formation and liver architecture. (**E**) Liver weight measurements across experimental groups to assess the impact of SLERT and HUNK expression on liver mass. ***$p < 0.001$. (**F**) Quantification of liver metastasis percentage from histological sections to determine the effect of SLERT on metastatic spread. ***$p < 0.001$. (**G**) Proposed model depicting SLERT's interaction with RBM15 and its effect on HUNK mRNA stability, influencing the PI3K/AKT pathway and promoting liver metastasis in colorectal cancer.

https://doi.org/10.2147/OTT.S514001

metastasis of colorectal cancer was influenced by factors such as angiogenesis and immune evasion; therefore, understanding SLERT's role in these processes was crucial.[26,27] Future research should explore how SLERT interacted with immune cells within the tumor microenvironment—potentially uncovering mechanisms by which it promoted immune escape or enhanced tumor vascularization.[28] Moreover, developing targeted therapies aimed at either inhibiting SLERT or restoring HUNK levels could have offered innovative strategies for mitigating colorectal cancer metastasis.[29,30] Such approaches might have involved designing small molecules or RNA-based therapies specifically targeting interactions between SLERT and RBM15 or enhancing HUNK stability. Despite advancements in treatment modalities for CRC, liver metastases continued to pose significant challenges regarding patient outcomes.[31,32] By elucidating the critical role played by SLERT in this process, our study laid the groundwork for targeted therapeutic strategies; inhibition of SLERT or restoration of HUNK expression may have presented novel avenues for reducing metastasis and improving survival rates among patients with colorectal cancer. These findings underscored an urgent need for further exploration into lncRNAs within cancer biology.[33–35] As our comprehension regarding non-coding RNAs continually expanded, lncRNAs held potential as integral components in both diagnosis and treatment paradigms related to cancer.[36] In conclusion, this study highlighted the essential function of SLERT in promoting liver metastasis associated with colorectal cancer through down-regulation of HUNK expression; additionally, its association with poor prognosis reinforced its viability as both a biomarker and therapeutic target.

Conclusion

In summary, this study reveals that the long non-coding RNA SLERT promotes liver metastasis in colorectal cancer by down-regulating HUNK expression. High SLERT levels correlate with poor patient prognosis, making it a potential diagnostic biomarker. SLERT disrupts the stabilizing effect of RBM15 on HUNK mRNA, enhancing metastatic potential. Targeting SLERT or restoring HUNK could provide new therapeutic strategies to improve outcomes in colorectal cancer.

Data Sharing Statement

The mRNA-seq data from this study have been submitted to the Gene Expression Omnibus (GEO) database, with accession codes GSE284657. The source data are available with the paper.

Author Contributions

All authors made a significant contribution to the work reported, whether that is in the conception, study design, execution, acquisition of data, analysis and interpretation, or in all these areas; took part in drafting, revising or critically reviewing the article; gave final approval of the version to be published; have agreed on the journal to which the article has been submitted; and agree to be accountable for all aspects of the work.

Funding

This study was funded by the Beijing Hope Run Special Fund of the Cancer Foundation of China (Grant No. LC2021A23), the Beijing Medical Award Foundation (Grant No. YXJL-2023-0670-0150), and the Beijing Science and Technology Medical Development Foundation (Grant No. KC2024-JX-0189).

Disclosure

The authors have no competing interests.

References

1. Morgan E, Arnold M, Gini A, et al. Global burden of colorectal cancer in 2020 and 2040: incidence and mortality estimates from GLOBOCAN. *Gut*. 2023;72(2):338–344. doi:10.1136/gutjnl-2022-327736
2. Siegel RL, Miller KD, Goding Sauer A, et al. Colorectal cancer statistics, 2020. *CA Cancer J Clin*. 2020;70(3):145–164. doi:10.3322/caac.21601
3. Crockett SD, Nagtegaal ID. Terminology, molecular features, epidemiology, and management of serrated colorectal Neoplasia. *Gastroenterology*. 2019;157(4):949–966.e944. doi:10.1053/j.gastro.2019.06.041
4. Engstrand J, Nilsson H, Strömberg C, Jonas E, Freedman J. Colorectal cancer liver metastases - a population-based study on incidence, management and survival. *BMC Cancer*. 2018;18(1):78. doi:10.1186/s12885-017-3925-x

5. Siebenhüner AR, Güller U, Warschkow R. Population-based SEER analysis of survival in colorectal cancer patients with or without resection of lung and liver metastases. *BMC Cancer*. 2020;20(1):246. doi:10.1186/s12885-020-6710-1
6. Nordlinger B, Sorbye H, Glimelius B, et al. Perioperative FOLFOX4 chemotherapy and surgery versus surgery alone for resectable liver metastases from colorectal cancer (EORTC 40983): long-term results of a randomised, controlled, Phase 3 trial. *Lancet Oncol*. 2013;14(12):1208–1215. doi:10.1016/S1470-2045(13)70447-9
7. Kanas GP, Taylor A, Primrose JN, et al. Survival after liver resection in metastatic colorectal cancer: review and meta-analysis of prognostic factors. *Clin Epidemiol*. 2012;4:283–301. doi:10.2147/CLEP.S34285
8. Zhou H, Liu Z, Wang Y, et al. Colorectal liver metastasis: molecular mechanism and interventional therapy. *Signal Transduct Target Ther*. 2022;7(1):70. doi:10.1038/s41392-022-00922-2
9. Tao B, Yi C, Ma Y, et al. A novel TGF-β-related signature for predicting prognosis, tumor microenvironment, and therapeutic response in colorectal cancer. *Biochem Genet*. 2024;62(4):2999–3029. doi:10.1007/s10528-023-10591-7
10. Lin D, Shen L, Luo M, et al. Circulating tumor cells: biology and clinical significance. *Signal Transduct Target Ther*. 2021;6(1):404.
11. Kron P, Lodge JPA. Changing perspectives in the treatment of colorectal liver metastases. *Br J Surg*. 2024;111(1). doi:10.1093/bjs/znad431
12. Wang Y, Zhong X, He X, et al. Liver metastasis from colorectal cancer: pathogenetic development, immune landscape of the tumour microenvironment and therapeutic approaches. *J Exp Clin Cancer Res*. 2023;42(1):177. doi:10.1186/s13046-023-02729-7
13. Kim JS, Kim H, Lee SY, et al. Hepatic arterial infusion in combination with systemic chemotherapy in patients with hepatic metastasis from colorectal cancer: a randomized Phase II study - (NCT05103020) - study protocol. *BMC Cancer*. 2023;23(1):691. doi:10.1186/s12885-023-11085-w
14. Jiang Y, Shao T, Zhao M, Xue Y, Zheng X. A network meta-analysis of efficacy and safety for first-line and maintenance therapies in patients with unresectable colorectal liver metastases. *Front Pharmacol*. 2024;15:1374136. doi:10.3389/fphar.2024.1374136
15. Xing YH, Yao RW, Zhang Y, et al. SLERT regulates DDX21 rings associated with pol i transcription. *Cell*. 2017;169(4):664–678.e616. doi:10.1016/j.cell.2017.04.011
16. Zhao D, Liu W, Chen K, Wu Z, Yang H, Xu Y. Structure of the human RNA polymerase I elongation complex. *Cell Discov*. 2021;7(1):97. doi:10.1038/s41421-021-00335-5
17. Fu Y, Liu Y, Wen T, et al. Real-time imaging of RNA polymerase I activity in living human cells. *J Cell Biol*. 2023;222(1). doi:10.1083/jcb.202202110.
18. Tian J, Cheng H, Wang N, Wang C. SLERT, as a novel biomarker, orchestrates endometrial cancer metastasis via regulation of BDNF/TRKB signaling. *World J Surg Oncol*. 2023;21(1):27. doi:10.1186/s12957-022-02821-w
19. Yan Q, Zhu C, Guang S, Feng X. The functions of non-coding RNAs in rRNA regulation. *Front Genet*. 2019;10:290. doi:10.3389/fgene.2019.00290
20. Wu M, Xu G, Han C, et al. lncRNA SLERT controls phase separation of FC/DFCs to facilitate Pol I transcription. *Science*. 2021;373(6554):547–555. doi:10.1126/science.abf6582
21. Yeh ES, Belka GK, Vernon AE, Chen CC, Jung JJ, Chodosh LA. Hunk negatively regulates c-myc to promote Akt-mediated cell survival and mammary tumorigenesis induced by loss of Pten. *Proc Natl Acad Sci U S A*. 2013;110(15):6103–6108. doi:10.1073/pnas.1217415110
22. Yeh ES, Abt MA, Hill EG. Regulation of cell survival by HUNK mediates breast cancer resistance to HER2 inhibitors. *Breast Cancer Res Treat*. 2015;149(1):91–98. doi:10.1007/s10549-014-3227-9
23. Zhang Y, Geng X, Li Q, et al. m6A modification in RNA: biogenesis, functions and roles in gliomas. *J Exp Clin Cancer Res*. 2020;39(1):192. doi:10.1186/s13046-020-01706-8
24. Wang R, Gao X, Xie L, Lin J, Ren Y. METTL16 regulates the mRNA stability of FBXO5 via m6A modification to facilitate the malignant behavior of breast cancer. *Cancer Metab*. 2024;12(1):22. doi:10.1186/s40170-024-00351-5
25. Diao MN, Zhang XJ, Zhang YF. The critical roles of m6A RNA methylation in lung cancer: from mechanism to prognosis and therapy. *Br J Cancer*. 2023;129(1):8–23. doi:10.1038/s41416-023-02246-6
26. Dudley AC, Griffioen AW. The modes of angiogenesis: an updated perspective. *Angiogenesis*. 2023;26(4):477–480. doi:10.1007/s10456-023-09895-4
27. Imodoye SO, Adedokun KA. EMT-induced immune evasion: connecting the dots from mechanisms to therapy. *Clin Exp Med*. 2023;23(8):4265–4287. doi:10.1007/s10238-023-01229-4
28. Kahn BM, Lucas A, Alur RG, et al. The vascular landscape of human cancer. *J Clin Invest*. 2021;131(2). doi:10.1172/JCI136655.
29. Han X, Jiang S, Gu Y, et al. HUNK inhibits epithelial-mesenchymal transition of CRC via direct phosphorylation of GEF-H1 and activating RhoA/LIMK-1/CFL-1. *Cell Death Dis*. 2023;14(5):327. doi:10.1038/s41419-023-05849-2
30. Reed KR, Korobko IV, Ninkina N, et al. Hunk/Mak-v is a negative regulator of intestinal cell proliferation. *BMC Cancer*. 2015;15(1):110. doi:10.1186/s12885-015-1087-2
31. Adam R, Piedvache C, Chiche L, et al. Liver transplantation plus chemotherapy versus chemotherapy alone in patients with permanently unresectable colorectal liver metastases (TransMet): results from a multicentre, open-label, prospective, randomised controlled trial. *Lancet*. 2024;404(10458):1107–1118. doi:10.1016/S0140-6736(24)01595-2
32. Cervantes A, Adam R, Roselló S, et al. Metastatic colorectal cancer: ESMO Clinical Practice Guideline for diagnosis, treatment and follow-up. *Ann Oncol*. 2023;34(1):10–32. doi:10.1016/j.annonc.2022.10.003
33. Kadian LK, Verma D, Lohani N, et al. Long non-coding RNAs in cancer: multifaceted roles and potential targets for immunotherapy. *Mol Cell Biochem*. 2024;479(12):3229–3254. doi:10.1007/s11010-024-04933-1
34. Wu W, He J. Unveiling the functional paradigm of exosome-derived long non-coding RNAs (lncRNAs) in cancer: based on a narrative review and systematic review. *J Cancer Res Clin Oncol*. 2023;149(16):15219–15247. doi:10.1007/s00432-023-05273-1
35. Zhang XZ, Liu H, Chen SR. Mechanisms of long non-coding RNAs in cancers and their dynamic regulations. *Cancers (Basel)* 2020;12(5):1245. doi:10.3390/cancers12051245
36. Saleh RO, Al-Ouqaili MTS, Ali E, et al. lncRNA-microRNA axis in cancer drug resistance: particular focus on signaling pathways. *Med Oncol*. 2024;41(2):52. doi:10.1007/s12032-023-02263-8